Journal of Dental Sciences 20 (2025) 1699–1708

Available online at www.sciencedirect.com

ScienceDirect

journal homepage: www.e-jds.com

Original Article

Effects of 3D-printers and manufacturer-specified post-curing units on the dimensional accuracy, compressive strength, and degree of conversion of resin for fixed dental prostheses

Citra Dewi Sahrir [a], Wei-Shao Lin [b], Ching-Shuen Wang [a], Hwai-En Lin [c], Chin-Wei Wang [a,d**], Wei-Chun Lin [e,f*]

[a] School of Dentistry, College of Oral Medicine, Taipei Medical University, Taipei, Taiwan
[b] Department of Prosthodontics, Indiana University School of Dentistry, Indianapolis, IN, USA
[c] Department of Mechanical Engineering, National Taipei University of Technology, Taipei, Taiwan
[d] Division of Periodontics, Department of Dentistry, Taipei Medical University Hospital, Taipei, Taiwan
[e] School of Dental Technology, College of Oral Medicine, Taipei Medical University, Taipei, Taiwan
[f] Department of Dentistry, Wan-Fang Hospital, Taipei Medical University, Taipei, Taiwan

Received 5 March 2025; Final revision received 20 March 2025
Available online 4 April 2025

KEYWORDS
3D-printer;
Post-curing;
Accuracy;
Compressive strength;
Resin polymerization

Abstract *Background/purpose:* The 3D printer and post-curing unit are important factors in producing the best 3D printed crowns. To explore the effects of different combinations of 3D-printers and manufacturer-specified post-curing units on the dimensional accuracy, compressive strength, and degree of conversion (DC%) of 3D-printable resin for fixed dental prostheses.
Materials and methods: Specimens were designed in 2 sizes and additively-manufactured using 2 digital light processing (DLP) 3D-printers (NextDent 5100, ND and PrintinDLP+, PN). The 3D-printed samples were polymerized using 2 different post curing units (LC-3D Print box, N and PrintInCure+, P). Dimensional accuracy was evaluated under an optical microscope, while compressive strength was determined using a universal testing machine. Fourier transform infrared spectroscopy was used to analyze the resin molecular bond characteristics and DC %. Statistical analysis, including ANOVA and Tukey's HSD post-hoc tests ($P < 0.05$).
Results: Significant dimensional variations were observed for both square and rectangular samples ($P < 0.001$). The ND-P showed the greatest ductility and relatively high maximum stress.

* Corresponding author. School of Dental Technology, College of Oral Medicine, Taipei Medical University, No. 250, Wu-Xing Street, Taipei, 11031, Taiwan.
** Corresponding author. School of Dentistry, College of Oral Medicine, Taipei Medical University, No. 250, Wu-Xing Street, Taipei, 11031, Taiwan.
E-mail addresses: jeffwa@tmu.edu.tw (C.-W. Wang), weichun1253@tmu.edu.tw (W.-C. Lin).

https://doi.org/10.1016/j.jds.2025.03.024

The fracture strengths were ND-N: 181.55 ± 8.37 MPa, ND-P: 151.54 ± 2.06 MPa, PN-N: 175.51 ± 12.44 MPa, and PN-P: 127.84 ± 10.10 MPa ($P < 0.001$). Surface inspection at 200 × magnification revealed subtler fault lines in ND-N and PN-P. FTIR analyses confirmed DC% was highest for ND-N (79.70 ± 1.02%) and PN-N (78.12 ± 0.94%), intermediate for ND-P (73.24 ± 0.89%) and PN-P (71.06 ± 1.67%).

Conclusion: Post-curing units had a greater impact on dimensional accuracy, strength, and polymerization than the choice of 3D-printer. Optimal resin properties require careful optimization of post-curing parameters and equipment.

Introduction

The progression of 3D-printing offers time-saving advantages for both dentists and patients.[1] The 3D-printing plays a pivotal role in the fabrication of dental casts and prostheses.[2–5] In addition to dimensional accuracy, fracture resistance is crucial. Although 3D-printed dental prostheses have the potential to fracture under a single strong load, but they are especially susceptible to damage from repeated loading. Consequently, it is essential for 3D-printed fixed dental prostheses (FDP) to possess mechanical properties that offer resistance to the stresses of repeated chewing.[6] The strength of the resin used in 3D printing is determined both by the energy absorbed from the light source during the printing process, which affects dimensional accuracy,[7,8] and by the post-processing light source energy, which enhances polymerization between resin monomers to ensure sufficient strength to withstand bite forces.[9,10]

Several factors can affect the dimensional accuracy and mechanical properties of 3D-printed dental prostheses during the manufacturing process, including printing orientation, post-curing, removal of supporting structures and finishing.[11] It has been shown that the post-curing unit and process are also significant influencing factors.[12,13] The post-curing procedure is vital because it aims to increase the degree of conversion (DC%), indicating the extent to which the polymer resin has undergone a chemical reaction and transformed into a solid polymer during the 3D-printing process.[14] A higher DC% results in a lower amount of residual monomer and better mechanical properties. Therefore, the setting of the 3D-printer and post-curing protocol have a major impact on the accuracy and mechanical strength of the printed prosthesis. Among the various types of 3D-printers, digital light processing (DLP) ones are considered the most suitable for dental applications due to their superior accuracy and faster 3D-printing time.[15,16] The inadequate post-curing of light-polymerizing resin can lead to high toxicity, while over-curing can negatively impact its mechanical properties.[17] Typically, each 3D-printer has specific manufacturer guidelines for post-curing and pos-processing procedures.[18] When using 3D-printers and post-curing unit from different manufacturers, careful consideration is required to achieve optimal properties of 3D-printed prostheses.

Several previous studies have employed compressive strength testing and fourier transform infrared spectroscopy (FTIR) to evaluate strength and degree of polymerization of resins.[19,20] The application of 3D-printed resins has been increasingly adopted in dental clinics. However, the diverse combinations of 3D printers and post-curing units have posed challenges for dentists and dental technicians in selecting appropriate equipment. Low-strength 3D-printed resins may fail to withstand the occlusal forces generated during mastication, leading to the fracture of restorations. Therefore, the primary goal is to optimize the combination of printing equipment to fabricate resin restorations with high accuracy and strength. This study aimed to explore the effects of different DLP 3D-Printers and manufacturer-specified post-curing units on the dimensional accuracy, compressive strength, and DC% of 3D-printed FDP resin. It was hypothesized that different DLP 3D printers and manufacturer-specified post-curing units did affect the dimensional accuracy, compressive strength, or DC% of 3D-printed FDP resin.

Materials and methods

The study design is shown in Figs. 1 and 2. The study specimens were designed in the standard shape using a computer-aided design (CAD) software (Solidworks 2018; Dassault Systèmes SE, Vélizy-Villacoublay, France), in dimensions of 10.0 × 10.0 × 1.2 mm (Square) and 25.0 × 2.0 × 2.0 mm (Rectangle), according to the specifications outlined the standard evaluation norm (ISO 10477) (Fig. 2A).[21] The designs were exported in standard tessellation language (STL) format and used for 3D-printed specimens using one DLP 3D-printer (NextDent 5100; NextDent, Soesterberg, The Netherlands) (ND) and another DLP 3D-printer (PrintinDLP+; Printin 3D, Taoyuan, Taiwan) (PN) (Fig. 3A and B). A commercially available FDP resin material (C&B resin; NextDent, Soesterberg, Netherlands) was used to fabricate all study samples. Previous studies indicated that a 0° printing angle yielded stable printing outcomes.[22] Therefore, the 3D-printing parameters were set to a 0° build orientation, a layer thickness of 50 μm, and a wavelength of 405 nm (Table 1). The 3D-printed samples were removed from the build platform and placed in an ultrasonic machine (Elmasonic Easy; Elma) containing 90% alcohol.

The samples were vibrated twice, for 5 min each time, to ensure thorough cleaning. Post-curing of samples was

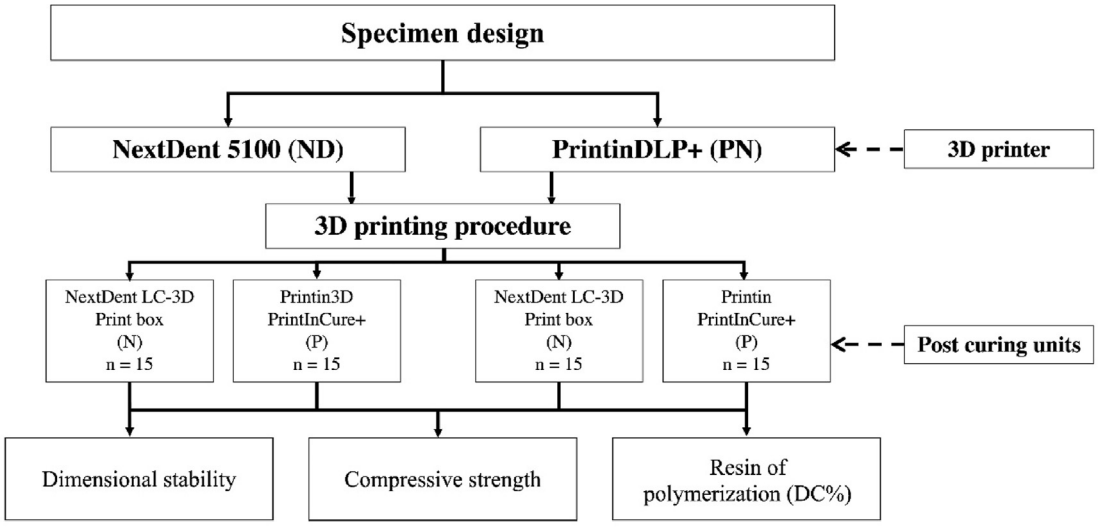

Figure 1 The workflow and research design of the entire experimental process.

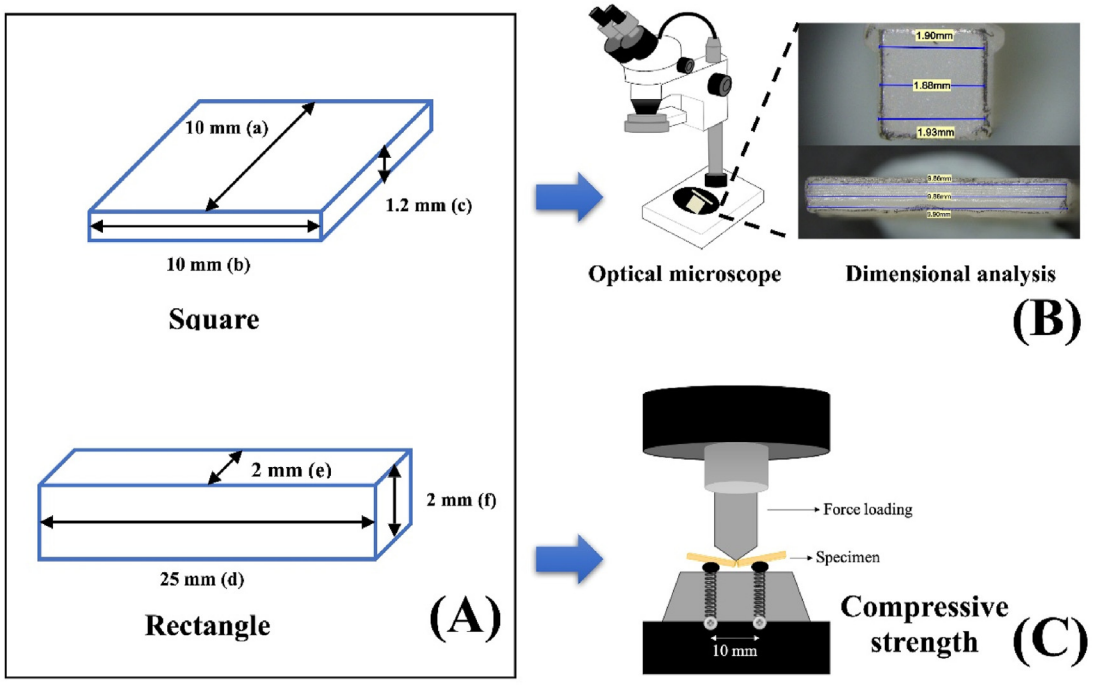

Figure 2 Illustration of preparation of this study: (A) Specimen samples showing the evaluated dimensions, (B) Size analysis, (C) Test design for measurement of fracture load.

performed using 2 different curing units: (N) an ultraviolet curing unit (LC-3D Print box; NextDent, Utrecht, The Netherlands) with a direct exposure time of 30 min (Fig. 3A and C), and (P) an ultraviolet curing unit (PrintInCure+; Printin, Taoyuan, Taiwan) with an exposure time of 15 min per side, totalling 30 min (Fig. 3B and D). The main technical features of the light-curing units are shown in Table 1.

The dimensions of the 3D-printed samples were measured using an optical microscope (Leica-Flexacam C1; Heerbrugg, Switzerland). Two sets of samples (n = 15) were used: a square sample with dimensions of 10.0 × 10.0 × 1.2 mm (denoted as a × b × c) and a rectangular sample with dimensions of 25.0 × 2.0 × 2.0 mm (denoted as d × e × f) along the X, Y, and Z axes. Each sample was analyzed under 10 × magnification. A scale bar of 1000 μm is shown in (Fig. 2B).

Each specimen was stored at 37 °C for 24 h according to the ISO 10477 standard before testing.[21] The rectangular samples (n = 15) with dimensions of 25.0 × 2.0 × 2.0 mm were used. A universal testing machine (AGX-V; Shimadzu, Kyoto, Japan) was employed to measure the fracture load, applying a vertical load at 1 mm/min until the sample fractured (Fig. 2C). Surface fractures were analyzed using a scanning electron microscope (SEM, Hitachi S-2400; Tokyo,

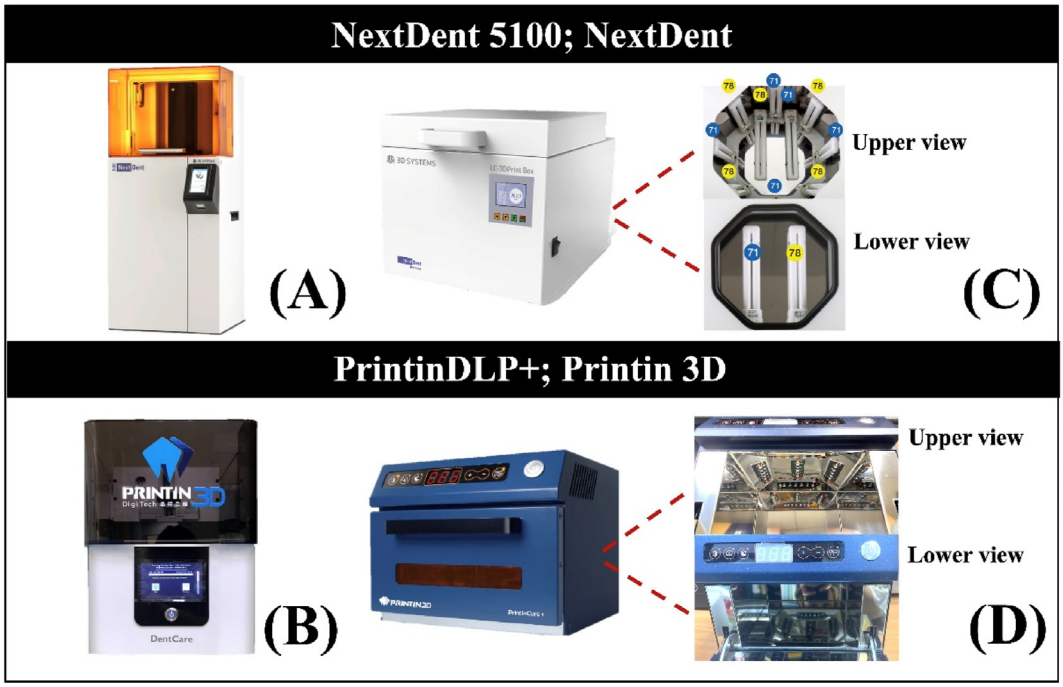

Figure 3 The different 3D printers and post-curing companies are as follows: (A) NextDent 5100, (B) PrintinDLP+, (C) LC-3D Print boX and (D) PrintInCure+.

Table 1 Study group design and the characteristics of 3D-printers and post-curing units.

Group		ND-N	ND-P	PN-N	PN-P
3D-printer	Manufacturer	NextDent	NextDent	Printin 3D	Printin 3D
	Machine type	NextDent 5100	NextDent 5100	PrintinDLP+	PrintinDLP+
	Technology	DLP	DLP	DLP	DLP
	Layer thickness (μm)	50	50	50	50
	Resolution (μm)	65	65	58	58
	Wavelength (nm)	405	405	405	405
Post-curing unit	Manufacturer	NextDent	Printin 3D	NextDent	Printin 3D
	Machine type	LC-3D Print box	PrintInCure+	LC-3D Print box	PrintInCure+
	Power supply (Vac/Hz)	240/50-60	240/50-60	240/50-60	240/50-60
	Power consumption (w)	264	70	264	70
	Fuse (A)	5.0	2.0	5.0	2.0
	Wavelength (nm)	365	405	365	405
	Exposure time (min)	30	15(2)	30	15(2)

Japan). Gold coating was applied to the fractured samples for 60 s to enhance their conductivity for SEM imaging. The interaction between the electron beam and the sample's surface facilitated the creation of detailed images.

Fourier transform infrared (FTIR) spectroscopy (Nicolet 8700; Thermo Scientific, Waltham, MA, USA) was used to analyze the functional groups and DC% in 3D-printed dental resin specimens. The scanning range for this analysis spanned from 400 to 4000 cm^{-1}, with a spectral resolution of 4 cm^{-1}, and each spectrum was obtained through 64 scans. The DC% was calculated by comparing the ratio of the carbon double bond peaks at two frequencies: the aliphatic stretching frequency at 1700 cm^{-1} and the reference aromatic frequency at 1644 cm^{-1}.[23,24] Degree of conversion (DC%) was calculated using the following formula.[24]

$$DC\% = \left[1 - \left[\frac{\left(\frac{1700\,cm^{-1}}{1644\,cm^{-1}}\right) peak\ hights\ after\ polymerization}{\left(\frac{1700\,cm^{-1}}{1644\,cm^{-1}}\right) peak\ hights\ before\ polymerization}\right]\right] \times 100$$

The sample size calculation was performed using G*Power software (version 3.1.9.6; Heinrich-Heine-Universität Düsseldorf), indicating that 15 samples per factor

combination in the 2 × 2 design would be sufficient to detect these differences with adequate power, ensuring robust estimates for both main effects and interaction effects. The collected data were analyzed using a statistical software (JMP 16 software; SAS). For each test result, the mean and standard deviation (SD) were calculated. The Shapiro–Wilk test was applied to assess the normality of the data. To determine statistical significance, a one-way analysis of variance (ANOVA) was conducted, followed by Tukey's honest significant difference (HSD) post-hoc test to identify specific differences between groups. Statistical significance was set at $P < 0.05$.

Results

The dimensional analysis for each group is presented in Table 2. For the square samples on the x axis surface (a), the dimensions ranged from 9.84 ± 0.13 mm to 9.99 ± 0.07 mm ($P < 0.001$). On the y axis surface (b), the dimensions ranged from 9.99 ± 0.04 mm to 10.18 ± 0.16 mm ($P < 0.001$). For the z axis surface (c), the dimensions ranged from 1.15 ± 0.06 mm to 1.23 ± 0.02 mm ($P < 0.001$). For the rectangular shape, the x axis surface (d) had dimensions ranging from 24.83 ± 0.04 mm to 25.22 ± 0.12 mm ($P < 0.001$). The y axis surface (e) showed dimensions ranging from 1.96 ± 0.03 mm to 2.05 ± 0.04 mm ($P < 0.001$). Finally, the z axis surface (f) had dimensions ranging from 1.89 ± 0.10 mm to 2.10 ± 0.07 mm ($P < 0.001$).

Fig. 4 illustrated the mechanical performance of 4 sample conditions. ND-N and PN-N exhibited higher maximum stress, indicating greater strength, whereas ND-P and PN-P displayed lower values, suggesting reduced mechanical performance. ND-P exhibited greater elongation before failure, reflecting higher ductility, while ND-N fractured at a lower strain, indicating brittleness. The ND-P group exhibited the highest ductility, with a displacement of approximately 1.6 mm and a relatively high maximum stress (151.54). Table 3 presented the fracture strength for ND-N, ND-P, PN-N, and PN-P, which were 181.55 ± 8.37 MPa, 151.54 ± 2.06 MPa, 175.51 ± 12.44 MPa, and 127.84 ± 10.10 MPa, respectively ($P < 0.001$). Additionally, PN-P was significantly lower from all other groups ($P < 0.001$).

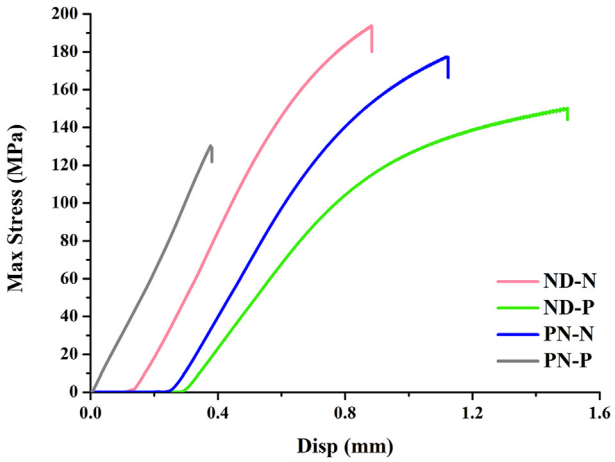

Figure 4 Maximal force curves were utilized to assess the compressive strength. ND-N: NextDent 5100 and LC-3D Print box. ND-P: NextDent 5100 and PrintInCure+. PN-N: PrintinDLP+ and LC-3D Print box. PN-P: PrintinDLP+ and PrintInCure+.

At 200 × magnification, the surfaces of the ND-N and PN-P samples revealed a similar topography, characterized by subtle and less discernible fault lines, suggesting a relatively uniform surface structure at this level of magnification. Closer examination showed that the fault lines on both the ND-P and PN-N samples were notably continuous, with rough edges and step-like external borders (Fig. 5). Further analysis revealed visible crack formations across all samples, with varying degrees of propagation. The cracks observed in the ND-P and PN-P samples were more pronounced, exhibiting increased continuity and depth, whereas those in the ND-N and PN-N samples appeared more localized with limited propagation. In particular, cracks measuring approximately

Table 2 The dimensional accuracy analysis of this study. All measurements are in mm.

Shape	Original size		ND-N	ND-P	PN-N	PN-P	*P* value
Square	Mean (SD)		Mean (SD)	Mean (SD)	Mean (SD)	Mean (SD)	
	a (x)	10.00	9.90 ± 0.08^{AB}	9.96 ± 0.06^{A}	9.99 ± 0.07^{A}	9.84 ± 0.13^{B}	<0.001[a]
	b (y)	10.00	9.99 ± 0.04^{B}	10.01 ± 0.03^{B}	10.18 ± 0.16^{A}	9.99 ± 0.03^{B}	<0.001[a]
	c (z)	1.20	1.15 ± 0.06^{B}	1.20 ± 0.04^{AB}	1.23 ± 0.02^{A}	1.20 ± 0.06^{AB}	<0.001[a]
Rectangle	d (x)	25.00	24.96 ± 0.14^{B}	25.16 ± 0.2^{A}	25.22 ± 0.12^{A}	24.83 ± 0.04^{B}	<0.001[a]
	e (y)	2.00	1.96 ± 0.03^{C}	1.99 ± 0.05^{C}	2.05 ± 0.04^{A}	2.00 ± 0.01^{B}	<0.001[a]
	f (z)	2.00	1.95 ± 0.07^{BC}	1.89 ± 0.10^{C}	2.02 ± 0.03^{AB}	2.10 ± 0.07^{A}	<0.001[a]

ND-N: NextDent 5100 and LC-3D Print box.
ND-P: NextDent 5100 and PrintInCure+.
PN-N: PrintinDLP+ and LC-3D Print box.
PN-P: PrintinDLP+ and PrintInCure+.
SD: Standard deviation.
Different capital letters indicate differences between group.
[a] *P* = Indicates significant difference ($P < 0.05$).

Table 3 Compressive strength (MPa) in mean.

Group	Mean	SD	Lower 95%	Upper 95%	F Ratio	*P* value
ND-N	181.55[A]	8.37	176.91	186.19	109.10	< 0.001[a]
ND-P	151.54[B]	2.06	150.40	152.69		
PN-N	175.51[A]	12.44	168.62	182.41		
PN-P	127.84[C]	10.10	122.25	133.44		

ND-N: NextDent 5100 and LC-3D Print box.
ND-P: NextDent 5100 and PrintInCure+.
PN-N: PrintinDLP+ and LC-3D Print box.
PN-P: PrintinDLP+ and PrintInCure+.
SD: Standard deviation.
Different capital letters indicate differences between group.
[a] *P* =Indicates significant difference ($P < 0.05$).

360–400 μm in length were clearly observed in the ND-P and PN-P samples.

The FTIR spectrum of the samples revealed their chemical composition through the identification of various functional groups (Fig. 6 and Table 4). The ND-N sample displayed a prominent peak at 3371 cm^{-1}, indicative of O–H stretching.[25,26] All samples exhibited peaks at 2942 cm^{-1} and 2874 cm^{-1}, corresponding to C–H stretching.[26] The peak at 1700 cm^{-1} and 1644 cm^{-1}, observed across all samples, were characteristic of C=O stretching.[27,28] The peak at 1533 cm^{-1} was attributed to C=C bonds.[28] In addition, the peaks ranging from 1242 cm^{-1} to 1037 cm^{-1}, confirmed the presence of C–O stretching.[25,27] The FTIR spectral analysis was further interpreted by comparing peak heights, using DC% values corresponding to wave numbers 1700 cm^{-1} and 1644 cm^{-1}. The mean and standard deviation of DC% for the ND-N, ND-P, PN-N, and PN-P groups were calculated as 79.70 ± 1.02%, 73.24 ± 0.89%, 78.12 ± 0.94%, and 71.06 ± 1.67%, respectively (Table 5) ($P < 0.001$).

Discussion

This study selected products from two manufacturers that utilized the same integrated 3D printing system for comparison. These systems included software, a 3D printer, a post-curing unit, and materials. This approach aimed to investigate the impact of cross-utilizing equipment from different systems on the properties of the resin. The null hypothesis was not rejected. The different DLP 3D-printers and manufacturer-specified post-curing units influenced the dimensional accuracy, compressive strength, and degree of conversion (DC%) of 3D-printed FDP resin. Regarding dimensional accuracy, the deviation between samples in each group ranged from 0.08 mm to 0.39 mm. However, the greatest deviation from the standard dimensions was observed in the x-axis of the rectangular shape in the PN-N group (0.22 mm). Dimensional deviations in other orientations ranged from 0 mm to 0.18 mm. In this study, the x-axis dimension of the Rectangle shape was the largest, measuring 25.00 mm. This may explain why the dimensional error increased as the sample size grew. Furthermore, variations in layer thickness, representing the z-axis resolution, did not affect the accuracy of either shape of the samples. This finding aligns with the report by Sim et al., which demonstrated that a smaller layer height, or shorter z-axis, does not always result in higher accuracy.[29] Staffova et al. also reported that sample thicknesses ranging from 2 to 5 mm had no significant effect on accuracy.[30] This study used a DLP 3D-printer, where the resolution is dictated by the pixel size. The presence of shadow areas between pixels leads to suboptimal polymerization in those regions, resulting in increased anisotropy of the 3D-printed objects. This effect is more pronounced when compared to other types of 3D-printers, such stereolithography (SLA) 3D-printers.[25,26] The anisotropy observed in DLP 3D-printers can be eliminated by post-curing.[31]

Occlusal force is influenced by various factors, such as dental and periodontal status, presence of a dental

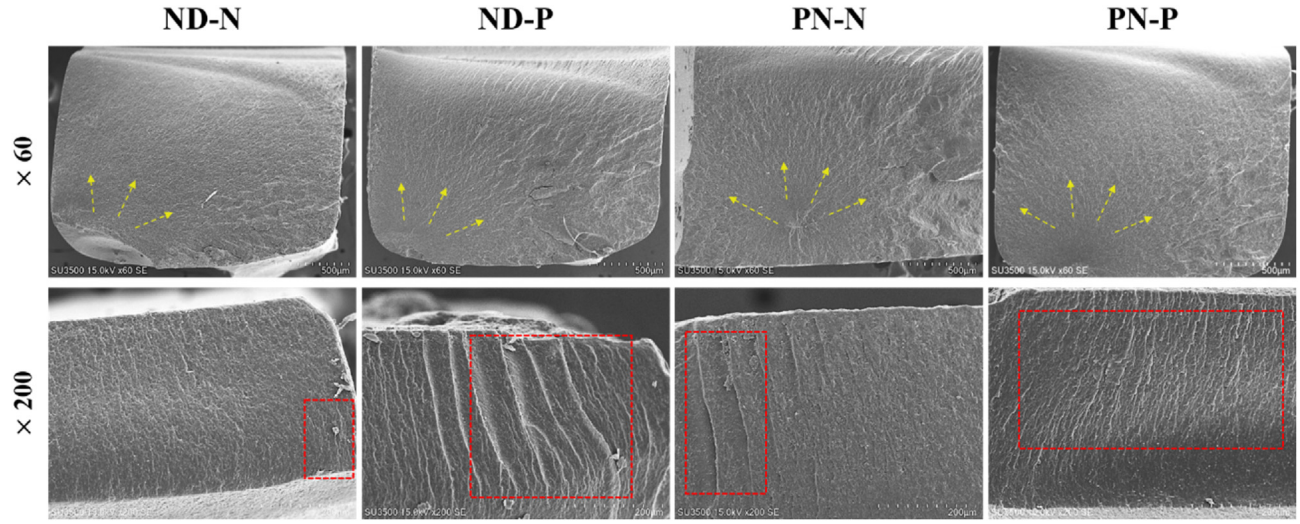

Figure 5 Representative SEM images after loading test. Yellow arrows indicated the crack origin and the direction of crack propagation, while red boxes highlighted the fracture lines. ND-N: NextDent 5100 and LC-3D Print box. ND-P: NextDent 5100 and PrintInCure+. PN-N: PrintinDLP+ and LC-3D Print box. PN-P: PrintinDLP+ and PrintInCure+

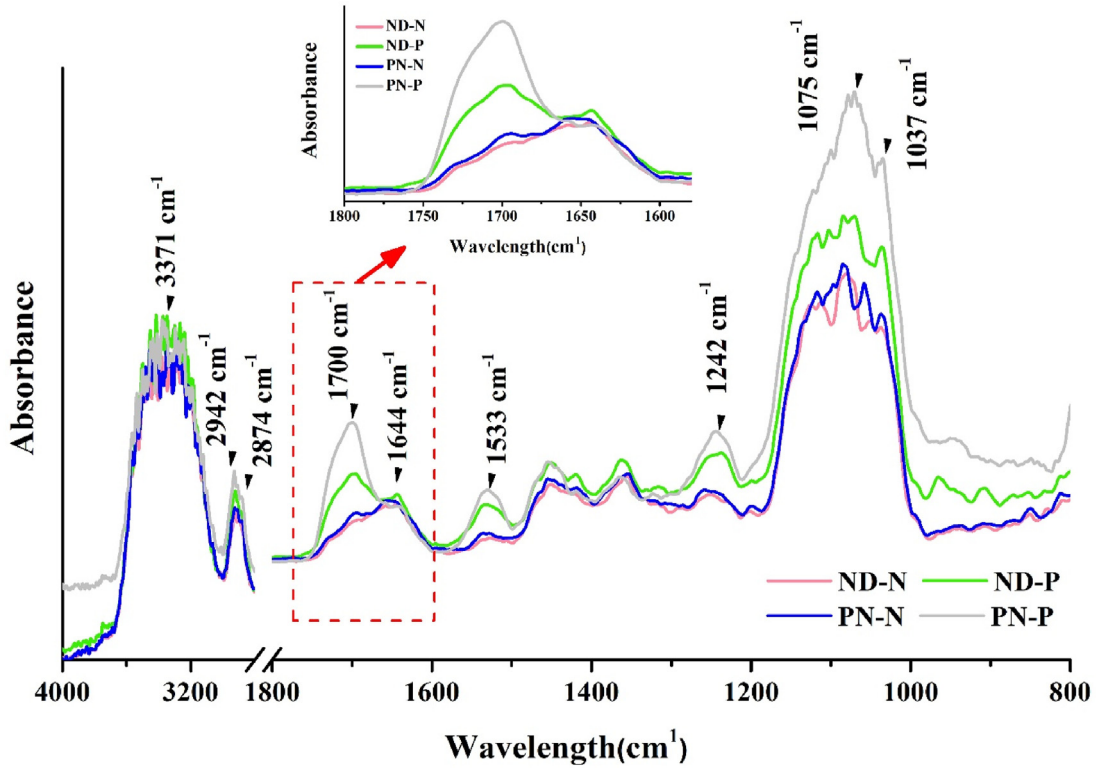

Figure 6 The attenuated total reflectance-fourier transform infrared spectroscopy (ATR-FTIR). ND-N: NextDent 5100 and LC-3D Print box. ND-P: NextDent 5100 and PrintInCure+. PN-N: PrintinDLP+ and LC-3D Print box. PN-P: PrintinDLP+ and PrintInCure+.

Table 4 Links of FTIR peaks at different locations.

Location (cm^{-1})	Represent	Reference
1037	C—O	25, 27
1075		
1242		
1533	C=C	28
1644	C=O	27, 28
1700		
2874	C—H	26
2942		
3371	O—H	25, 26

C—O: Carbon—oxygen bond.
C=C: Carbon—carbon double bond.
C=O: Carbonyl group.
C—H: Carbon—hydrogen bond.
O—H: Hydroxyl group.

Table 5 Degree of conversion (DC%) for 3D-printed resin.

Group	Mean (DC %)	SD	F Ratio	*P* value
ND-N	79.70^{A}	1.02	59.37	<0.001[a]
ND-P	73.24^{B}	0.89		
PN-N	78.12^{A}	0.94		
PN-P	71.06^{C}	1.67		

ND-N: NextDent 5100 and LC-3D Print box.
ND-P: NextDent 5100 and PrintInCure+.
PN-N: PrintinDLP+ and LC-3D Print box.
PN-P: PrintinDLP+ and PrintInCure+.
SD: Standard deviation.
SD: Standard deviation.
Different capital letters indicate differences between group.
[a] *P* =Indicates significant difference ($P < 0.05$).

prosthesis and age.[32,33] Similarly, the strength of 3D-printing resin can be enhanced through one or more of the following factors: build orientation, the addition of filler or nanofiller, post-polymerization time and temperature, and layer thickness.[34] The results presented in Fig. 4 and Table 3 suggest that matched 3D-printers and manufacturer-specified post-curing units may not necessarily improve 3D-printing outcomes. Notably, the ND-N group exhibited the highest strength, at 181.55 MPa, demonstrating that consistent use of a 3D-printer and post-curing unit yields superior performance compared to other groups. In contrast, the PN-P group recorded the lowest strength, at 127.84 MPa, indicating increased brittleness. It appears that one post-curing unit (N: LC-3D Print Box; NextDent), with a direct exposure time of 30 min, outperformed the other post-curing unit (P: PrintInCure+; Printin). Despite these variations, all tested materials demonstrated strengths greater than 50 MPa, which is clinically acceptable for polymer crowns.[35] Enkhjargal Bayarsaikhan et al. reported the effects of post-curing temperature on the mechanical properties of 3D-printed dental resin materials.[21] Their findings indicated that variations in curing temperature and irradiation time altered the resin's compressive strength, which ranged from 100.70 ± 6.65 MPa to 147.48 ± 5.82 MPa. Although PN-P (127.84 ± 10.10 MPa) exhibited the lowest strength among the tested groups, it still demonstrated a

relatively good performance compared to the values reported in the literature.

The effects of different post-curing equipment on the resin were further analyzed by observing the microstructure of the resin's fracture surface. At all SEM magnifications, fractography shows similar fracture patterns in samples 3D-printed and post-cured with both same (ND-N, PN-P) and different (ND-P, PN-N) manufacturers. At 200 × magnification, ND-N and PN-P exhibit uniform surfaces with subtle fault lines, while ND-P and PN-N display continuous fault lines with rough, step-like edges. The origins of surface cracks may be attributed to the internal stress generated during the printing and post-curing processes. The polymerization shrinkage of the resin, combined with thermal and light-induced curing stresses, likely contributed to crack initiation. In ND-P and PN-P, the post-curing process may have induced uneven polymerization, leading to stress concentration at weak points and resulting in more extensive crack propagation. Conversely, the relatively localized cracks in ND-N and PN-N suggest a lower degree of residual stress, potentially due to differences in printing parameters or the absence of additional post-curing effects. This study identified the fracture origin on the tension side of the lower surface of the bar sample (Fig. 5), consistent with the findings of Alghazzawi et al. The crack initiates from the bottom corner of the bar.[36] Garofalo et al. also confirmed that the fracture origin is located on the tensile side of the buckling bar.[37] In 3D-printed crowns, cracks may originate at the point of load application, propagating from the tensile zone on the intaglio surface to the outer part of the crown.[38] The overall results support the hypothesis that characteristic fracture features vary based on the 3D-printer manufacturer and the post-curing process used.

Incomplete polymerization can reduce the bond strength between polymer chains, while thorough polymerization promotes the formation of a strong and homogeneous material.[39] FTIR analysis was performed to measure DC% and determine functional groups. The ND-N sample displayed a prominent peak at 3371 cm^{-1}, indicative of O—H stretching, suggesting a substantial presence of hydroxyl groups, possibly from alcohols or phenols.[26] All samples exhibited peaks at 2942 cm^{-1} and 2874 cm^{-1}, corresponding to C—H stretching, confirming the presence of alkyl groups.[23,26] A peak at 1700 cm^{-1} and 1644 cm^{-1} indicated C═O stretching, suggesting carbonyl groups.[27] Peaks at 1533 cm^{-1} for C═C stretching are associated with amine or imine rings.[28] Peaks at 1242 cm^{-1}, 1075 cm^{-1}, and 1037 cm^{-1} indicated C—O stretching, characteristic of alcohols, ethers, or esters.[27] A study by Kirby et al. demonstrated that the choice of alternative light-curing units did not have a statistically significant effect on the DC% of 3D-printed dental models.[14] Similarly, no significant differences in DC% were observed with varying curing times.[24]

Furthermore, research by Bayarsaikhan et al. found that temperature variations did not significantly impact DC% outcomes.[21] However, no previous studies have investigated the relationship between the DC% and the various combinations of 3D-printers and post-curing units. Table 5 shows that ND-N and PN-N have higher DC%, indicating a greater degree of polymerization. This higher DC% reflects increased conversion of double bonds into carbonyl-containing products, signifying more extensive polymerization. In contrast, ND-P and PN-P exhibit lower DC%, likely due to the superior performance of another post-curing unit. Dong Wu et al. reported the effects of the ultraviolet post-curing process on printed resins.[40] The results showed that the uneven distribution of light exposure could have caused material warping and variations in DC%. Therefore, similar to the findings of this study, differences in light-curing machines led to variations in exposure conditions. The addition of a light source at the bottom of the LC-3D Print Box, compared to the PrintInCure+, may have been a key factor in enhancing the DC%. Therefore, the hypothesis of this study was not rejected, suggesting that different DLP 3D printers and post-curing units did affect the dimensional accuracy, compressive strength, or DC% of 3D-printed FDP resin.

With the advancement of dental technology, numerous manufacturers had introduced various 3D printing devices and materials. However, clinical guidelines did not provide clear recommendations on selecting the appropriate steps for dental 3D printing. Dentists and dental technicians typically considered several factors when purchasing equipment, including printing quality, cost, brand, ease of operation, and device size. However, 3D printing equipment was not restricted to a single system or manufacturer, which further complicated the selection of 3D printers and post-curing units. Based on the findings of this study, the post-curing unit played a critical role in influencing the properties of 3D-printed resin. Therefore, clinical operators were advised to select an appropriate post-curing unit based on the specific resin material used in order to achieve optimal resin restorations.

This study was limited to specific combinations of 3D printers and curing units. Future studies will continue to explore the effects of light source positioning and light attenuation in different post-curing units on the degree of conversion of 3D-printed resins. The post-curing unit demonstrated a more pronounced effect on dimensional accuracy, compressive strength, and DC% than the choice of the 3D printer. Achieving optimal properties in 3D-printing resin requires thorough optimization of post-curing parameters and equipment.

Declaration of competing interest

The authors have no conflicts of interest relevant to this article.

Acknowledgments

This research is partially supported by the Young Yushan Fellow Program by the Ministry of Education (MOE), Taiwan (112-2001-012-400) to Chin-Wei Wang. Thanks to PrintIn3D DigiTech Co., LTD for providing the 3D printing equipment and assisting with sample production. Thanks to POPLAR Co., LTD the Taiwan agent of NextDent, for providing the NextDent equipment and assisting with sample production.

References

1. Alotaibi K, Kassim A. Digitization in dentistry: a conceptual framework for digital dental technologies and dental

informatics in dental practice. *Int J Intell Syst Appl Eng* 2023; 11:965—74.
2. Beleges EM, Khurayzi TA, Dallak SA, et al. Applications of 3D printing in restorative dentistry: the present scenario. *Saudi J Oral Dent* 2021;6:15—21.
3. Sahrir CD, Ruslin M, Lee SY, Lin WC. Effect of various post-curing light intensities, times, and energy levels on the color of 3D-printed resin crowns. *J Dent Sci* 2024;19:357—63.
4. Gupta H, Bhateja S, Arora G. 3D printing and its applications in oral and maxillofacial surgery. *IP J Surg Allied Sci* 2019;1:48—52.
5. Zarbah M, Aldowah O, Alqahtani NM, et al. Dimensional stability of 3D-printed edentulous and fully dentate hollowed maxillary models over periods of time. *BMC Oral Health* 2024; 24:495.
6. Park S, Cho W, Lee H, et al. Strength and surface characteristics of 3D-printed resin crowns for the primary molars. *Polymers* 2023;15:4241.
7. Butler N, Zhao Y, Lu S, Yin S. Effects of light exposure intensity and time on printing quality and compressive strength of β-TCP scaffolds fabricated with digital light processing. *J Eur Ceram* 2024;44:2581—9.
8. Kang MJ, Lim JH, Lee CG, Kim JE. Effects of post-curing light intensity on the mechanical properties and three-dimensional printing accuracy of interim dental material. *Materials* 2022; 15:6889.
9. Bayarsaikhan E, Gu H, Hwangbo NK, et al. Influence of different postcuring parameters on mechanical properties and biocompatibility of 3D printed crown and bridge resin for temporary restorations. *J Mech Behav Biomed Mater* 2022;128: 105127.
10. Tian Y, Chen C, Xu X, et al. A review of 3d printing in dentistry: technologies, affecting factors, and applications. *Scanning* 2021;2021:9950131.
11. Caussin E, Moussally C, Le Goff S, et al. Vat photopolymerization 3D printing in dentistry: a comprehensive review of actual popular technologies. *Materials* 2024;17:950.
12. Alzahrani SJ, Hajjaj MS, Azhari AA, Ahmed WM, Yeslam HE, Carvalho RM. Mechanical properties of three-dimensional printed provisional resin materials for crown and fixed dental prosthesis: a systematic review. *Bioengineering* 2023;10:663.
13. Gad MM, Fouda SM. Factors affecting flexural strength of 3D-printed resins: a systematic review. *J Prosthodont* 2023;32: 96—110.
14. Kirby S, Pesun I, Nowakowski A, França R. Effect of different post-curing methods on the degree of conversion of 3D-printed resin for models in dentistry. *Polymers* 2024;16:549.
15. Shin SH, Lim JH, Kang YJ, Kim JH, Shim JS, Kim JE. Evaluation of the 3D printing accuracy of a dental model according to its internal structure and cross-arch plate design: an in vitro study. *Materials* 2020;13:5433.
16. Ryu JE, Kim YL, Kong HJ, Chang HS, Jung JH. Marginal and internal fit of 3D printed provisional crowns according to build directions. *J Adv Prosthodont* 2020;12:225—32.
17. Guttridge C, Shannon A, O'Sullivan A, O'Sullivan K, O'Sullivan W. Biocompatible 3D printing resins for medical applications: a review of marketed intended use, biocompatibility certification, and post-processing guidance. *Ann 3D Print Med* 2022;5:100044.
18. Revilla-León M, Özcan M. Additive manufacturing technologies used for processing polymers: current status and potential application in prosthetic dentistry. *J Prosthodont* 2019;28: 146—58.
19. Nel HA, Chetwynd AJ, Kelly CA, et al. An untargeted thermogravimetric analysis-fourier transform infrared-gas chromatography-mass spectrometry approach for plastic polymer identification. *Environ Sci Technol* 2021;55:8721—9.
20. Campanale C, Savino I, Massarelli C, Uricchio VF. Fourier transform infrared spectroscopy to assess the degree of alteration of artificially aged and environmentally weathered microplastics. *Polymers* 2023;15:911.
21. Bayarsaikhan E, Lim JH, Shin SH, et al. Effects of postcuring temperature on the mechanical properties and biocompatibility of three-dimensional printed dental resin material. *Polymers* 2021;13:1180.
22. Lu TY, Lin WC, Yang TH, Sahrir CD, Shen YK, Feng SW. The influence of dental virtualization, restoration types, and placement angles on the trueness and contact space in 3D-printed crowns: a comprehensive exploration. *Dent J* 2024; 12:2.
23. Sahrir CD, Lin WS, Wang CW, Lin WC. Effects of post-curing light intensity on the trueness, compressive strength, and resin polymerization characteristics of 3D-printed 3-unit fixed dental prostheses. *J Prosthodont* 2024 (in press).
24. Altarazi A, Haider J, Alhotan A, Silikas N, Devlin H. Assessing the physical and mechanical properties of 3D printed acrylic material for denture base application. *Dent Mater* 2022;38: 1841—54.
25. Cobb JS, Zai-Rose V, Correia JJ, Janorkar AV. FT-IR Spectroscopic analysis of the secondary structures present during the desiccation induced aggregation of elastin-like polypeptide on silica. *ACS Omega* 2020;5:8403—13.
26. Nandiyanto ABD, Ragadhita R, Fiandini M. Interpretation of fourier transform infrared spectra (FTIR): a practical approach in the polymer/plastic thermal decomposition. *Indones J Sci Technol* 2023;8:113—26.
27. Brza MA, Aziz SB, Anuar H, Al Hazza MHF. From green remediation to polymer hybrid fabrication with improved optical band gaps. *Int J Mol Sci* 2019;20:3910.
28. Bhatia L, Sahu DK. SEM & FTIR analysis of rice husk to assess the impact of physiochemical pretreatment. *J Agric Ecol Res Int* 2023;24:1—13.
29. Sim MY, Park JB, Kim DY, Kim HY, Park JM. Dimensional accuracy and surface characteristics of complete-arch cast manufactured by six 3D printers. *Heliyon* 2024;10:e30996.
30. Štaffová M, Ondreáš F, Svatík J, Zbončák M, Jančář J. 3D printing and post-curing optimization of photopolymerized structures: basic concepts and effective tools for improved thermomechanical properties. *Polym Test* 2022;108:107499.
31. Lee J, Ju S, Kim J, Hwang S, Ahn J. The comparison of the accuracy of temporary crowns fabricated with several 3D printers and a milling machine. *J Adv Prosthodont* 2023;15: 72—9.
32. Kaur H, Singh N, Gupta H, et al. Effect of various malocclusion on maximal bite force- a systematic review. *J Oral Biol Craniofac Res* 2022;12:687—93.
33. Pantea M, Ciocoiu RC, Greabu M, et al. Compressive and flexural strength of 3D-printed and conventional resins designated for interim fixed dental prostheses: an in vitro comparison. *Materials* 2022;15:3075.
34. Gad MM, Fouda SM. Factors affecting flexural strength of 3D-printed resins: a systematic review. *J Prosthodont* 2023;32: 96—110.
35. Atria PJ, Bordin D, Marti F, et al. 3D-printed resins for provisional dental restorations: comparison of mechanical and biological properties. *J Esthetic Restor Dent* 2022;34: 804—15.
36. Alghazzawi TF, Janowski GM, Ning H, Eberhardt AW. Qualitative SEM analysis of fracture surfaces for dental ceramics and polymers broken by flexural strength testing and crown compression. *J Prosthodont* 2023;32:100—10.
37. Garófalo SA, Wehner M, Dohrn A, et al. Increasing dental zirconia micro-retentive aspect through ultra-short pulsed laser

microstructuring: study on flexural strength and crystal phase characterization. *Clin Oral Invest* 2022;26:939—55.
38. Refaie A, Bourauel C, Fouda AM, Keilig L, Singer L. The effect of cyclic loading on the fracture resistance of 3D-printed and CAD/CAM milled zirconia crowns-an in vitro study. *Clin Oral Invest* 2023;27:6125—33.
39. Kim RJY, Kim DH, Seo DG. Post-polymerization of three-dimensional printing resin using a dental light curing unit. *J Dent Sci* 2024;19:945—51.
40. Wu D, Zhao Z, Zhang Q, Qi HJ, Fang D. Mechanics of shape distortion of DLP 3D printed structures during UV post-curing. *Soft Matter* 2019;15:6151—9.